Pharmacokinetics, Dosimetry, and Toxicity of the Targetable Atomic Generator, ^{225}Ac-HuM195, in Nonhuman Primates

Matthias Miederer, MD[1]; Michael R. McDevitt, PhD[1]; George Sgouros, PhD[2]; Kim Kramer, MD[3]; Nai-Kong V. Cheung, MD, PhD[3]; and David A. Scheinberg, MD, PhD[1]

[1]Department of Molecular Pharmacology and Chemistry, Memorial Sloan-Kettering Cancer Center, New York, New York; [2]Department of Radiology, John Hopkins University, Baltimore, Maryland; and [3]Department of Pediatrics, Memorial Sloan-Kettering Cancer Center, New York, New York

Short-lived α-emitting isotopes individually conjugated to monoclonal antibodies have now reached human use, but little is still known about their toxicity. Use of antibody targetable ^{225}Ac nanogenerators is a new approach in the field of α-immunotherapy offering the advantage of a 10-d half-life ($t_{1/2}$) and increased potency due to generation of 3 new atoms, yielding a total of 4 α-particles. However, the 3 α-emitting daughter elements generated have the potential for significant toxicity as these nuclides are no longer bound to the carrier IgG. **Methods:** Cynomolgus monkeys were used to evaluate the toxicity of prototype ^{225}Ac nanogenerators. Monoclonal antibody HuM195 (anti-CD33) is the carrier for planned human clinical trials of ^{225}Ac; there are no CD33 sites in cynomolgus monkeys. In one experiment, 2 monkeys received a single intravenous dose of ^{225}Ac-HuM195 at 28 kBq/kg. This dose level is approximately the planned initial human dose. In another experiment, 2 animals received a dose escalation schedule of 3 increasing ^{225}Ac-HuM195 doses with a cumulative activity of 377 kBq/kg. The whole-blood $t_{1/2}$ of ^{225}Ac, ratios of ^{225}Ac to its ultimate α-emitting daughter nuclide ^{213}Bi, generation of monkey anti-HuM195 antibodies (MAHA), hematologic indices, serum biochemistries, and clinical parameters were measured. Monkeys were euthanized and examined histopathologically when the dose escalation reached toxicity. **Results:** The blood $t_{1/2}$ of ^{225}Ac-HuM195 was 12 d, and 45% of generated ^{213}Bi daughters were cleared from the blood. MAHA production was not detected. Approximately 28 kBq/kg of ^{225}Ac caused no toxicity at 6 mo, whereas a cumulative dose of ~377 kBq/kg caused severe toxicity. In the cumulative dosing schedule, single doses of ~37 kBq/kg resulted in no toxicity at 6 wk. After ~130 kBq/kg were administered, no toxicity was observed for 13 wk. However, 28 wk after this second dose administration, mild anemia and increases of blood urea nitrogen and creatinine were detected. After administration of an additional 185 kBq/kg, toxicity became clinically apparent. Monkeys were euthanized 13 and 19 wk after the third dose administration (cumulative dose was 377 kBq/kg). Histopathologic evaluation revealed mainly renal tubular damage associated with interstitial fibrosis. **Conclusion:** ^{225}Ac nanogenerators may result in renal toxicity and anemia at high doses. The longer blood $t_{1/2}$ and the lack of target cell antigens in cynomolgus monkeys may increase toxicity compared with human application. Therefore, a dose level of at least 28 kBq/kg may be a safe starting dose in humans. Hematologic and renal function will require close surveillance during clinical trials.

Key Words: ^{225}Ac; radioimmunotherapy; α-particles; CD33; HuM195

J Nucl Med 2004; 45:129–137

Radioimmunotherapy is a promising approach to selectively treat a variety of cancers (*1,2*). It takes advantage of a growing number of monoclonal antibodies to target tumor cells preferentially while sparing normal, healthy tissue. This potentially increases the therapeutic index compared with other treatment modalities. Recent advances in chemistry have led to methods for stable conjugation of a variety of radionuclides, including both halogens and metals to proteins and peptides (*3–5*).

Radiation as a cytotoxic agent has several advantages over therapeutics that interfere chemically with their target cells. Most importantly, radiation is able to kill tumor tissue without the need for binding or internalization into every target cell. Second, combinations of radiotherapy with some chemotherapeutic approaches results in a more than additive therapeutic effect (*6*). Due to optimizations in external beam therapy, local control of many tumors is possible, whereas micrometastatic disease is currently amenable only to treatment with systemic chemotherapeutic agents. One important step toward feasible radiotherapeutic treatment of micrometastatic disease is to target radiation via monoclonal antibodies directly to tumor throughout the body. Commonly used isotopes for this are the β-emitting isotopes ^{131}I and ^{90}Y (*7*). Recently, several α-emitting isotopes such as ^{213}Bi and ^{211}At have been studied clinically as radioisotopes in cancer therapy (*3,8*). α-Particles are characterized by 400-fold greater linear energy transfer than β-particles.

Received May 28, 2003; revision accepted Sep. 25, 2003.

For correspondence or reprints contact: David A. Scheinberg, MD, PhD, Department of Molecular Pharmacology and Chemistry, Memorial Sloan-Kettering Cancer Center, 1275 York Ave., New York, NY 10021.

E-mail: d-scheinberg@ski.mskcc.org

UH & EURATOM Ex. 2021-001
Fusion v. Universität Heidelberg, et al.
IPR2023-00551

Whereas the β-particle's range is typically between 0.5 and 8 mm, α-particles have a tissue pathlength of only 40–90 μm. Therefore, α-radiation is suitable for killing single-cell diseases and small tumor cell clusters consisting only of a few thousand cells. One of the most potent, yet challenging, therapeutic α-emitting approaches is the use of an α-generator: ^{225}Ac. ^{225}Ac has the convenient half-life ($t_{1/2}$) of 10 d and decays via a chain, yielding a total of 4 α-particles. The α-emitting daughter nuclides are short-lived (^{221}Fr, $t_{1/2}$ = 4.8 min; ^{217}At, $t_{1/2}$ = 32.3 ms; ^{213}Bi, $t_{1/2}$ = 45.6 min), leading to an extremely high cytotoxicity when retained in or near tumor cells or tumor cell clusters. A key drawback of this same property is the release of the daughters from ^{225}Ac immunoconjugates; such daughters may not be retained in tumor tissue (*9*). Though used successfully in small animal systems, ^{225}Ac generators have not been used in humans (*10*).

In this study, we describe initial monkey studies of a new radioimmunoconjugate consisting of the α-emitting isotope ^{225}Ac conjugated to the anti-CD33 antibody HuM195. HuM195 is a humanized antibody that targets CD33 on acute myeloid leukemia cells. HuM195 has been used as the targeting moiety in a variety of clinical trials as a native antibody and conjugated to β-emitting and α-emitting isotopes (*8*).

The longest lived α-emitting daughter nuclide of ^{225}Ac is ^{213}Bi. Bismuth accumulates in renal tissue and, therefore, nephrotoxicity was hypothesized to be the dose-limiting toxicity in ^{225}Ac immunotherapy due to constant kidney accumulation of ^{213}Bi arising from systemic ^{225}Ac (*11*). Therefore, prior to human trials, we evaluated ^{225}Ac-HuM195 toxicity in a nonhuman primate model.

MATERIALS AND METHODS

Preparation of ^{225}Ac-HuM195

^{225}Ac was conjugated to HuM195 antibody using a 2-step labeling method as described previously (*12*). Briefly, labeling and preparation of the doses were done at the Memorial Sloan-Kettering Cancer Center (MSKCC) Central Isotope Laboratory to ensure consistency and to standardize each step for human clinical use. ^{225}Ac (37 MBq in 25 μL 0.2 mol/L HCl; Oak Ridge National Laboratory) was incubated with l-ascorbic acid (150 g/L, 20 μL), 2-(*p*-isothiocyanatobenzyl)-1,4,7,10-tetraazacyclododecane-1,4,7,10-tetraacetic acid (DOTA-NCS) (10 g/L, 50 μL; Macrocyclics), and tetramethylammonium acetate (2 mol/L, 50 μL; Aldrich Chemical Co.) to facilitate incorporation of ^{225}Ac into DOTA. The reaction was allowed to continue for 30 min at 60°C (pH 5.0). For conjugation of ^{225}Ac-DOTA to HuM195 (the second-step reaction), another 20 μL of ascorbic acid were added before adding 1 mg of HuM195 (200 μL; Protein Design Laboratories). The pH was adjusted with carbonate/bicarbonate buffer (1 mol/L, 100 μL) to 9.0 and incubation was for 30 min at 37°C. Afterward, free ^{225}Ac along with other metals was absorbed with 20 μL 10 mmol/L diethylenetriaminepentaacetic acid (DTPA) and the unconjugated ^{225}Ac was separated from ^{225}Ac-HuM195 by PD10 size exclusion (Bio-Rad) using 1% human serum albumin in 0.9% saline as eluent. Quality control of the final product included thin-layer chromatography to determine radiopurity, a cell-based binding assay to measure immunoreactivity of the antibody vehicle, *Limulus* amebocyte lysate testing to determine pyrogen content, and microbiologic culture in fluid thioglycollate of soybean-casein digest medium to verify sterility.

Nonhuman Primate Study Design

Four male cynomolgus monkeys, 2–4 y old, were used in this study. Housing and care were in accordance with the Animal Welfare Act and the *Guide for the Care and Use of Laboratory Animals* (*13*). Animal protocols were approved by the Institutional Animal Care and Use Committee at MSKCC. All procedures were performed under short-term intramuscular ketamine anesthesia.

In one experiment, 2 animals received a single intravenous dose of ^{225}Ac-HuM195 at 28 kBq/kg via femoral venipuncture. This dose level was scaled from 1/20 of the maximum tolerated dose values determined in rodents (*10*). With regard to the total number of α-particles emitted until total decay of the ^{225}Ac, this dose was similar to a ^{213}Bi dose that has proven safe in patients previously (*8*).

Animals were observed twice daily for levels of brightness, alertness, and reactivity and weighed weekly. Biochemical and hematologic indices of the blood (IDEXX Laboratory) as well as blood radioactivity values were determined on days 1, 5, 8, 14, and 18 and monthly thereafter.

In another experiment, 2 animals received a dose escalation schedule of 3 increasing ^{225}Ac-HuM195 doses (at 0, 6, and 34 wk) with a cumulative activity of ~370 kBq/kg, also administered by femoral venipuncture. Animals were followed similarly for laboratory values and for clinical toxicity.

Determination of Monkey Antihuman Antibodies

Monkey antihuman antibody production was assessed on days 6 and 12 after the first injection and on day 6 after the third injection in monkeys 3 and 4. Serum samples (100 μL) were incubated with 250 ng/mL ^{111}In-HuM195 for 10 min at room temperature and then the molecular weight of the radioactive fraction was determined using Beckman Coulter System Gold high-performance liquid chromatography (HPLC) equipped with a γ-RAM Radio HPLC detector (IN/US Systems, Inc.). Therefore, 50-μL samples were injected onto a size-exclusion column (300 × 7.8 mm TSK 3000SWXL; Supelco) and an elution profile was measured over 16 min. The mobile phase consisted of 0.15 mol/L sodium chloride/0.02 mol/L sodium acetate, pH 6.5. The sensitivity of the HPLC radiodetector and the ^{111}In-HuM195 antibody concentration allows accurate detection of monkey anti-HuM195 antibody (MAHA) titer above 50 ng/mL.

Histopathologic Evaluation

Necropsy was performed after euthanasia by barbiturate overdose. Tissues from the cerebrum, testis, salivary gland, skeletal muscle, esophagus, trachea, stomach, small intestine, spleen, lung, liver, adrenal grand, large intestine, and kidneys were stained with hematoxylin–eosin and examined by 2 veterinary pathologists.

Pharmacokinetic Analysis and Absorbed-Dose Estimation

Due to the concern of iatrogenic anemia, blood samples were kept to a minimum and only blood samples of ~1 mL were analyzed for blood activity level by γ-counting (Packard Cobra γ-Counter; Packard Instrument Co.). The blood pharmacokinetic data obtained in the ^{221}Fr and ^{213}Bi photon windows were used to estimate blood and renal cortex absorbed dose. Starting at 30 min

UH & EURATOM Ex. 2021-002
Fusion v. Universität Heidelberg, et al.
IPR2023-00551

after each blood drawing, blood activity was measured separately for ^{213}Bi and ^{221}Fr and measured several times thereafter until equilibration of the daughters. The steady-state ratio of ^{213}Bi to ^{221}Fr was back-extrapolated by using exponential growth of ^{213}Bi and constant activity of ^{221}Fr. Due to the 4.5-min $t_{1/2}$ of ^{221}Fr, its activity approximates ^{225}Ac after 25 min. In this way, time–activity curves for ^{225}Ac and ^{213}Bi were obtained separately.

The blood dose was obtained by fitting the ^{225}Ac time–activity curve to a 1-component (monkey 2) or 2-component (monkey 1) exponential expression. The resulting fitted expressions were analytically integrated over time to yield the total number of ^{225}Ac disintegrations occurring in the blood. Fitting was performed using the Simulation Analysis and Modeling software package, SAAM II (SAAM Institute, Inc.). Two different assumptions were then applied to estimate the number of ^{221}Fr and ^{217}At disintegrations in blood. In the first assumption, these 2 daughters were assumed to decay at the site of ^{225}Ac decay—that is, in the blood. In the second assumption, these daughters were assumed to decay at the site of ^{213}Bi decay. ^{213}Bi decays not occurring in the blood were assumed to occur in the kidneys, specifically the renal cortex portion of the kidneys. Once the decays of each radionuclide were apportioned to blood or the renal cortex of the kidneys, the absorbed dose was obtained assuming a uniform deposition of α-particle energy in the tissue mass. The energy emitted per disintegration was, therefore, multiplied by the number of disintegrations and by the α-particle energy emitted per disintegration; the result was then divided by the blood or renal cortex mass. The electron and photon energy contributions to the tissue absorbed dose were considered negligible relative to the α-particle energy and were, therefore, not included.

The number of ^{213}Bi disintegrations occurring in the blood was obtained separately by integrating, over time, the back-extrapolated estimate of ^{213}Bi radioactivity concentration in blood at each time. This provided an estimate of ^{213}Bi disintegrations occurring in the blood. The difference between the total number of ^{225}Ac disintegrations and the ^{213}Bi disintegrations—that is, those disintegrations resulting from ^{213}Bi that was no longer in the blood—was assigned to the renal cortex portion of the kidneys (*14*). The decay of an equal number of ^{221}Fr and ^{217}At was assigned to the blood (assumption A) or to the renal cortex of the kidneys (assumption B).

The mass of blood in cynomolgus monkeys was obtained as the product of 80 mL/kg and the total body weight of the monkeys (*15*). The mass of the renal cortex was obtained by assuming that the kidney mass of a 5-kg cynomolgus monkey is the same as that of a 5-kg (2–3 y old) human (*16*). The adult renal cortex-to-total kidney mass ratio (*17*) was then used to obtain the renal cortex mass.

RESULTS

Toxicity of Single-Dose ^{225}Ac-HuM195

At a dose level of 28 kBq/kg administered once intravenously, no clinical or laboratory toxicity was observed for >6 mo. Serum tests including hepatic enzymes (serum glutamic-oxalocetic transaminase, serum glutamic-pyruvic transaminase, alkaline phosphatase, γ-glutamyl transpeptidase, and bilirubin), renal values (blood urea nitrogen [BUN] and creatinine), hematology values (hemoglobin, red blood cell count, and white blood cell [WBC] count), and electrolytes (sodium, potassium, chloride, carbon dioxide, calcium, and phosphorus) were normal at all times. A nonspecific rise in serum creatine phosphokinase (CPK) was observed after intramuscular anesthesia. Independence of this finding from radioimmunoconjugate administration was shown by elevated CPK values after each handling, even if no drug was administered. The peak of CPK elevation was reproducibly observed 24 h after intramuscular ketamine anesthesia with significant elevation over 4–5 d.

Blood $t_{1/2}$ of ^{225}Ac-HuM195

The blood $t_{1/2}$ of ^{225}Ac-HuM195 in both monkeys was ~12 d. In monkey 1, biphasic pharmacokinetics were observed comprising a rapid clearing component with a $t_{1/2}$ of 2.3 ± 0.2 d and a slowly clearing component with a $t_{1/2}$ of 12 ± 1 d. In monkey 2, a single-component exponential fit demonstrated a $t_{1/2}$ of 12 ± 2 d (Fig. 1).

MAHA Detection

The engineered HuM195 is a potential immunogen in cynomolgus monkeys. Monkey antihuman antibody response (MAHA) could result in a major change in biodistribution of the second or third injection of ^{225}Ac-HuM195 compared with the first administration. In particular, it would be expected that if complexed by MAHA an increased percentage of ^{225}Ac-HuM195 would be cleared rapidly through the liver or spleen. HPLC of monkey sera incubated with ^{111}In-HuM195 showed no radioactive fraction at ≥300 kDa, indicating that the 2 monkeys injected with 3 doses of HuM195 did not generate neutralizing antibody against the human protein throughout the course of the study (Fig. 2).

Clinical Toxicity of ^{225}Ac-HuM195

Animals in the dose-escalating study showed no signs of toxicity 6 wk after administration of doses of 30 and 59

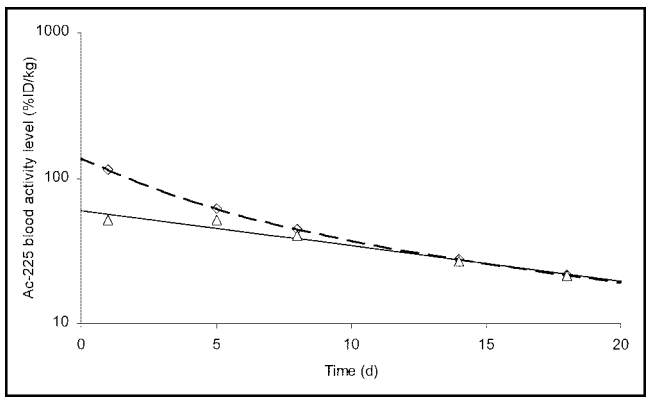

FIGURE 1. Blood time–activity curves of ^{225}Ac. Activity concentration for ^{225}Ac was estimated from ^{221}Fr counting after equilibration. Dashed line (monkey 1, ◇) corresponds to 2-component exponential fit to data. α-Component (42%) cleared with $t_{1/2}$ of 2.3 ± 0.2 d and slow β-component (58%) cleared with $t_{1/2}$ of 12 ± 1 d. Solid line (monkey 2, △) is single-component exponential fit with intercept and $t_{1/2}$ of 60.3 percentage injected dose per kilogram (%ID/kg) and 12 ± 2 d, respectively.

UH & EURATOM Ex. 2021-003
Fusion v. Universität Heidelberg, et al.
IPR2023-00551

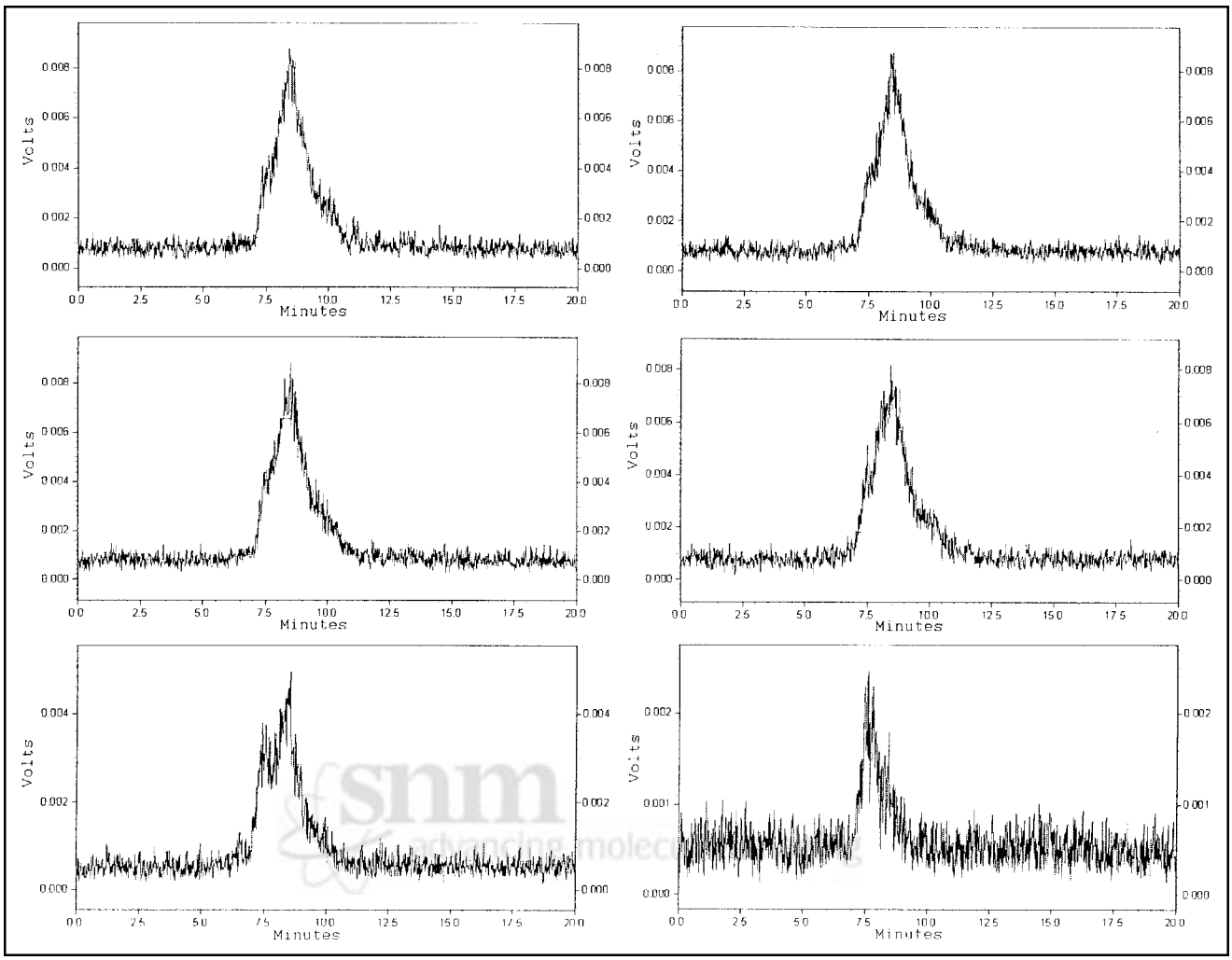

FIGURE 2. HPLC assay for monkey antihuman antibody response (MAHA). ^{111}In-HuM195 was incubated with monkey serum obtained 6 d after injection 1 (top row), 12 d after injection 1 (middle row), and 6 d after injection 3 (bottom row). Antibody dimers (300 kDa) or multimers (>450 kDa) suggestive of autoantibodies against HuM195 were not detected. Retention time of ~150-kDa HuM195 is 8.4 min. Higher molecular weight 300 kDa would have markedly shorter retention time (<6.4 min). (Left) Data for monkey 4. (Right) Data for monkey 3.

kBq/kg. The second dose at 133 and 130 kBq/kg (cumulative doses,163–189 kBq/kg) also did not result in any clinical toxicity for up to 3 additional months after administration. However, a trend toward decrease of hemoglobin levels was observed (Fig. 3). Anemia could have arisen from toxicity, such as decreased production of erythropoietin, hemolysis, or the repeated bleedings.

After a 4-mo hiatus, animals were reevaluated at the time of an additional injection. At time of administration of this third dose (215 and 189 kBq/kg; cumulative dose, 377 kBq/kg), 28 wk after administration of the second dose, evidence of renal failure with elevated creatinine levels (monkey 3, 1.6 mg/dL; monkey 4, 2.6 mg/dL) and worsening anemia (monkey 3, 7.3 mg/dL; monkey 4, 6.8 mg/dL) were observed. Therefore, the third dose was likely to be cleared slowly from the kidney and would likely compound the toxicity already present. Monkey 4 suffered from increasing anorexia, weight loss, and lethargy during the next 13 wk and was euthanized 47 wk after the first dose. Monkey 3 deteriorated clinically at a slower pace. He was euthanized at 1 y after the first dose, for histopathologic examination (Figs. 4 and 5). Marrow toxicity as measured by reduced WBC counts was not found to be a toxicity of ^{225}Ac-HuM195 (Fig. 6).

Histopathologic Examination

Monkey 4 showed histopathologic damage in renal tissue, but not elsewhere. This damage was characterized by multifocal proximal dilated convoluted tubules due to the loss of tubular epithelial cells. These tubules were also associated with interstitial fibrosis and, rarely, small aggregates of mononuclear cells in the interstitium (Fig. 7). Bone marrow was mildly hypocellular in the sternum and femur.

Monkey 3 showed histopathologic damage in a variety of other organs. Changes in renal lesions were less overt than

UH & EURATOM Ex. 2021-004
Fusion v. Universität Heidelberg, et al.
IPR2023-00551

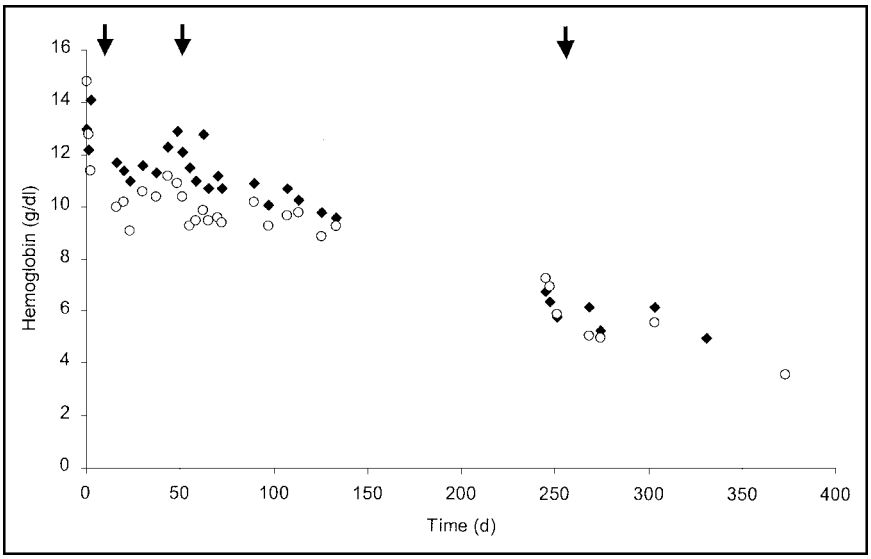

FIGURE 3. Hemoglobin levels in monkeys receiving dose escalation of ^{225}Ac-HuM195. Doses were given at weeks 0, 6, and 28. Arrows indicate time of intravenous injection of 0.15, 0.67, and 1.07 MBq in monkey 3 (○) and 0.3, 0.67, and 0.93 MBq in monkey 4 (◆).

in monkey 4 but were similar in nature. Some tubular epithelial necrosis and marked regeneration, corresponding to more chronic lesions, could be seen. Some interstitial fibrosis and hyaline casts were also noted (Fig. 7). Other organs showed histopathologic damage consistent either with radiation damage or with severe stress. Myocardial tissue showed areas of interstitial fibrosis and aggregates of mononuclear cells with degeneration of surrounding myocytes; the gastric mucosa showed many well-demarcated erosions; liver showed areas of mild hepatocellular degeneration and testis showed seminiferous tubular lumens containing multinucleated giant cells. Cellularity of bone marrow was moderately hypocellular in sternum and severely hypocellular in femur.

Pharmacokinetic Analysis and Absorbed Dose Estimation

Dose estimates were made based on the time–activity curves for ^{225}Ac (Fig. 1) and ^{213}Bi (Fig. 8). Steady-state in vivo ratios of ^{213}Bi to its parent nuclide ^{225}Ac was 0.57:1 ($\pm$0.11) in monkey 1 and 0.54:1 in monkey 2 ($\pm$0.13) (Figs. 8A and 8B). Tables 1 and 2 summarize the dosimetry results obtained under the 2 different assumptions described in the Materials and Methods. Blood and renal cortex absorbed doses were obtained by an extrapolation of kinetics measured for monkey 1 to monkey 3 and monkey 4, both of whom received a total of 1.89 MBq ^{225}Ac-HuM195. Under the assumption that ^{221}Fr and ^{217}At decay with the ^{225}Ac, the blood dose is 4 Gy and the renal cortex dose is 5 Gy.

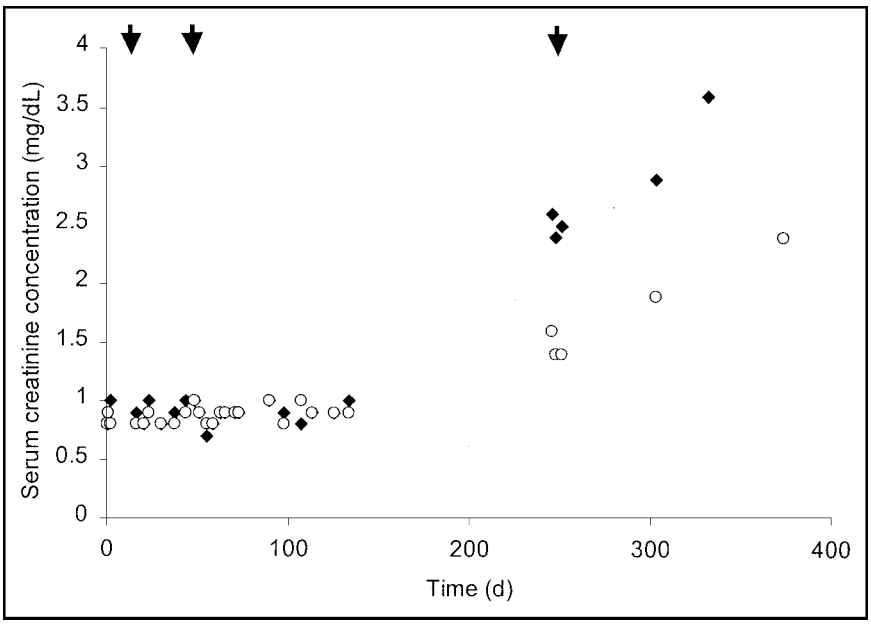

FIGURE 4. Serum creatinine levels in monkeys receiving dose escalation of ^{225}Ac-HuM195. Dose and schedule were as in Figure 3. Arrows indicate intravenous injection times. ○, Monkey 3; ◆, monkey 4.

UH & EURATOM Ex. 2021-005
Fusion v. Universität Heidelberg, et al.
IPR2023-00551

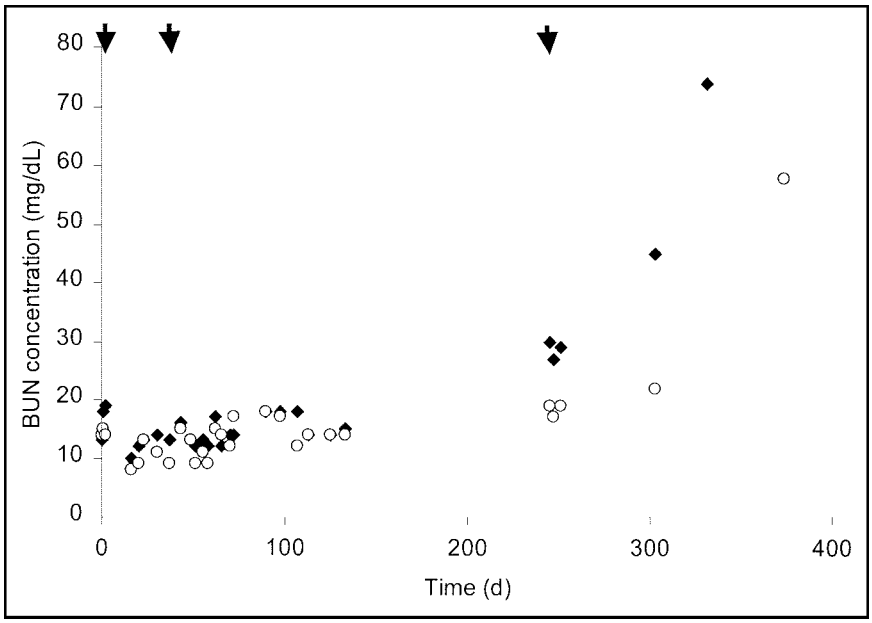

FIGURE 5. Serum BUN levels in monkeys receiving dose escalation of ^{225}Ac-HuM195. Dose and schedule were as in Figure 3. Arrows indicate intravenous injection times. ○, Monkey 3; ◆, monkey 4.

Assuming that the kinetics on monkey 2 apply, the blood dose is 3 Gy and the renal cortex dose is 3 Gy. Under the second assumption, that ^{221}Fr and ^{217}At decay with the ^{213}Bi, using kinetics of monkey 1, the blood dose is 3 Gy and the renal cortex dose is 13 Gy; using kinetics of monkey 2, the blood dose is 2 Gy and the renal cortex dose is 9 Gy.

DISCUSSION

Targeted ^{225}Ac represents a new class of drugs, which have not yet been used in humans (*10*). ^{225}Ac-HuM195 was developed as a highly cytotoxic α-radiation emitter targeted by specific binding to CD33 and internalization of the monoclonal antibody-generator construct. While several forms of radioimmunotherapy have been developed and used in humans, the unique features of targeted nanogenerators required that potential side effects be evaluated in primate studies before application in humans. ^{225}Ac has the unique property of decaying via an atomic chain containing 3 additional α-emitting isotopes, each with different chemical properties. We have shown that clinical grade ^{225}Ac-HuM195 production, quality control, and administration are feasible. In the future, the 10-d $t_{1/2}$ of ^{225}Ac will allow central production of ^{225}Ac immunoconjugates under controlled reproducible conditions and distribution to multiple sites of clinical application.

^{225}Ac labeling of HuM195 did not affect its immunoreactivity nor did labeling change the blood $t_{1/2}$ when compared with previous studies in monkeys using HuM195 (*18*). In addition, the chelated ^{225}Ac is stable in vivo. This suggests that metabolism will be determined primarily by

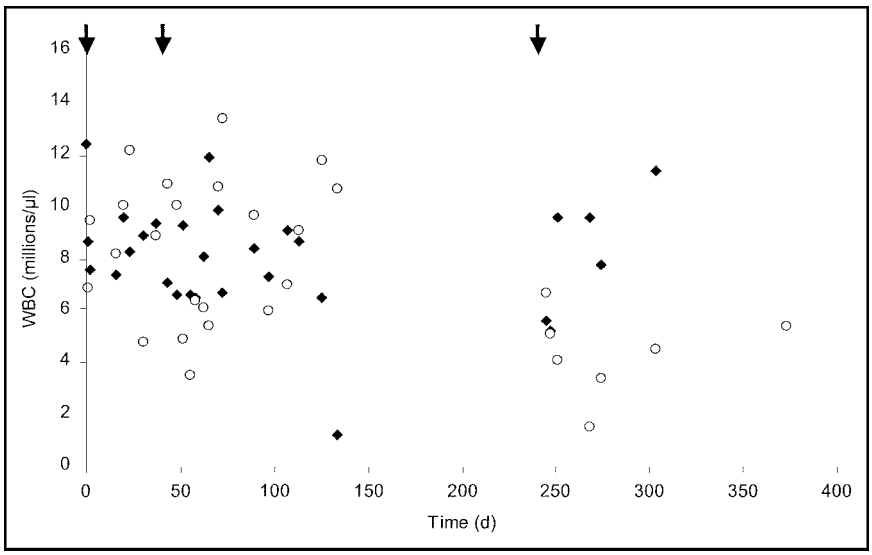

FIGURE 6. WBC counts in monkeys receiving dose escalation of ^{225}Ac-HuM195. Dose and schedule were as in Figure 3. Arrows indicate intravenous injection times. ○, Monkey 3; ◆, monkey 4.

UH & EURATOM Ex. 2021-006
Fusion v. Universität Heidelberg, et al.
IPR2023-00551

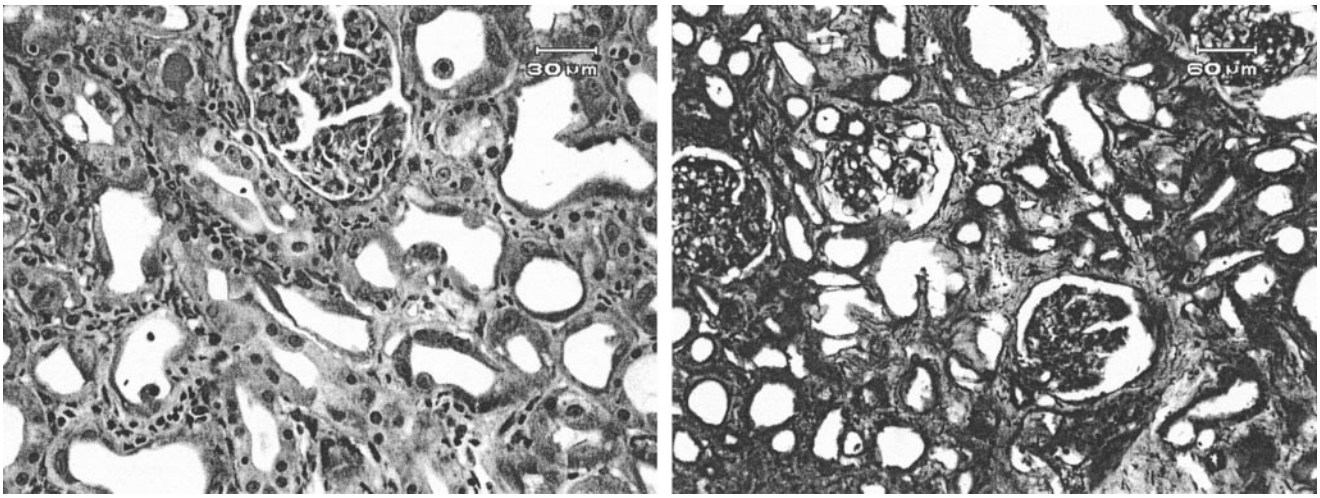

FIGURE 7. Histopathologic examination of kidneys taken after euthanasia of monkeys. Kidney damage was observed in different stages. (Left) Monkey 3 shows tubular necrosis and regeneration mixed with some interstitial fibrosis, indicative of more chronic damage. (Right) Monkey 4 also displays tubular damage and marked interstitial fibrosis in more acute state.

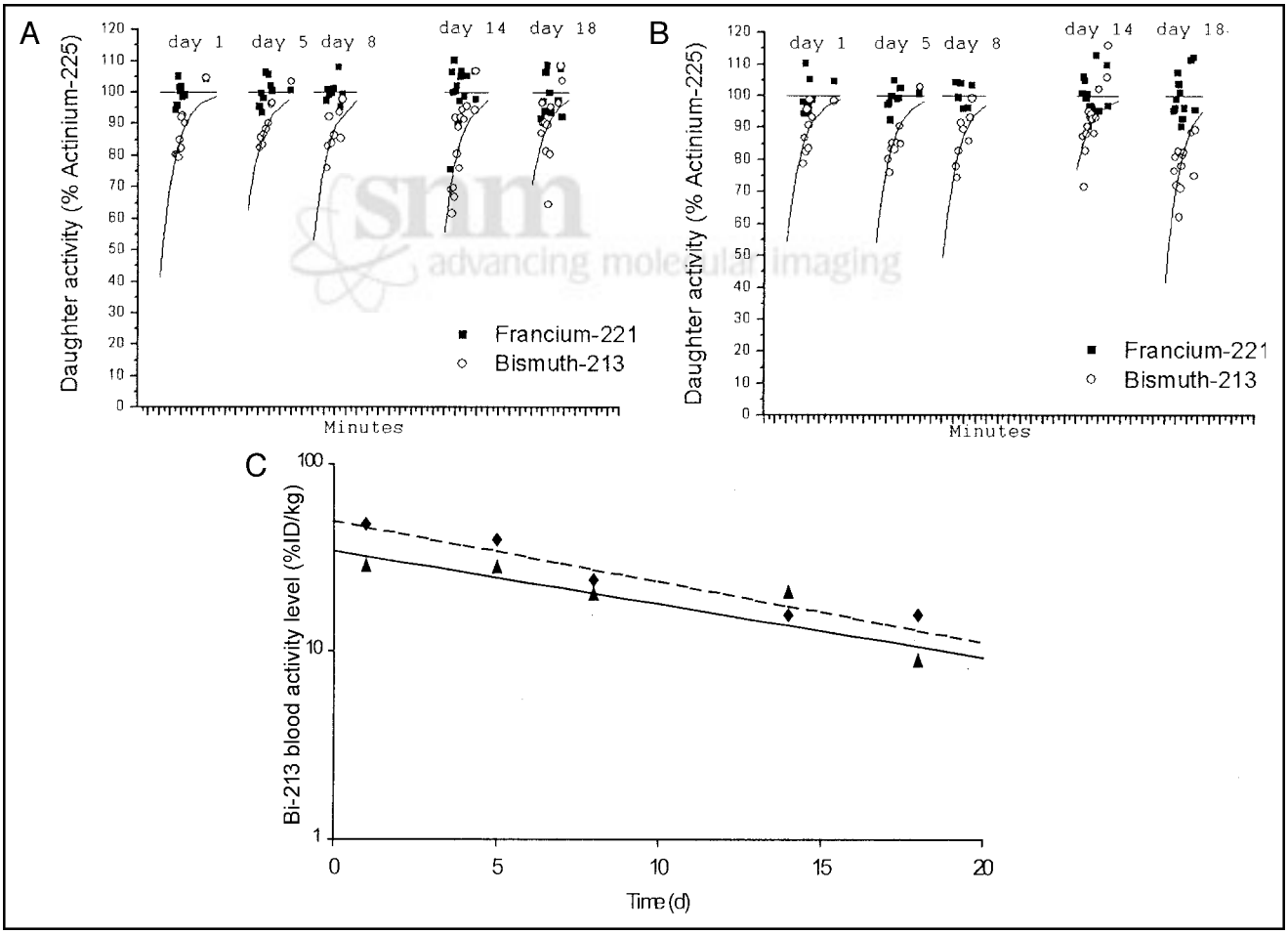

FIGURE 8. (A and B) Relationship between ^{213}Bi and ^{221}Fr activity in whole blood. Recorded activities of ^{213}Bi (○) and ^{221}Fr (■) in monkey 1 (A) and monkey 2 (B) are shown. Each individual small curve represents data from single day (days 1, 5, 8, 14, and 18, respectively, after ^{225}Ac-HuM195 administration). For each curve, *x*-axis is linear with respect to time during which isotope equilibrium is reached ex vivo. (C) Blood time–activity curves of ^{213}Bi. Activity concentration for ^{213}Bi was estimated by back-extrapolating ^{213}Bi counts to time of blood collection. Dashed line (monkey 1) corresponds to 1-component exponential fit with intercept and $t_{1/2}$ of 49 percentage injected dose per kilogram (%ID/kg) and 9 ± 2 d, respectively. Corresponding values for monkey 2 (solid line) are 34 %ID/kg and 11 ± 3 d, respectively.

UH & EURATOM Ex. 2021-007
Fusion v. Universität Heidelberg, et al.
IPR2023-00551

TABLE 1
Dosimetry of Single Dose of ^{225}Ac-HuM195 Following Pharmacokinetics in Monkey 1

	No. of disintegrations (/37 kBq)				Absorbed dose (Gy/37 kBq)			
	Blood (Bq-s/kg)		RC (Bq-s)		Blood		RC	
Isotope	A	B	A	B	A	B	A	B
^{225}Ac	2.2×10^{10}	2.2×10^{10}	0	0	0.020	0.020	0	0
^{221}Fr	2.2×10^{10}	1.1×10^{10}	0	4.8×10^{9}	0.022	0.011	0	0.08
^{217}At	2.2×10^{10}	1.1×10^{10}	0	4.8×10^{9}	0.025	0.012	0	0.08
^{213}Bi	1.1×10^{10}	1.1×10^{10}	4.8×10^{9}	4.8×10^{9}	0.015	0.015	0.10	0.10
Total	7.7×10^{10}	5.5×10^{10}	4.8×10^{9}	1.4×10^{10}	0.082	0.058	0.10	0.26

RC = renal cortex portion of kidney.
A and B refer to radionuclide decay assumptions A and B in text.

the carrier IgG and the physical properties of the radioisotopes. The blood $t_{1/2}$ of a monoclonal antibody is affected by specific recognition by the immune system or by binding to Fc receptors, thereby increasing clearance, and by specific binding to target cells. Monkeys do not express CD33. Therefore, HuM195 blood $t_{1/2}$ in monkeys is long (~12 d), whereas in patients displaying CD33 binding sites on both normal monocytes and leukemia cells it is far shorter (2–3 d) (*19,20*). In humans, after binding sites become saturated or leukemia cells are cytoreduced, blood $t_{1/2}$ increased (*18*). The biologic $t_{1/2}$ of monoclonal antibody and the physical half-life of the ^{225}Ac radioisotope are matched well. In contrast, the more commonly used short-lived α-emitting isotopes ^{213}Bi ($t_{1/2}$ = 46 min) and ^{211}At ($t_{1/2}$ = 7 h) demand more injections to maintain high blood activity concentrations. This results in a more complicated and expensive regimen and as well in accumulation of unlabeled, potentially blocking monoclonal antibodies over the course of the treatment.

Due to the short pathlength of α-radiation, unbound α-immunoconjugates circulating in blood are unlikely to cause significant toxicity. After the initial decay of ^{225}Ac to ^{221}Fr, however, this daughter α-emitting element, and the subsequent α-emitting daughters, ^{217}At and ^{213}Bi, would be released. The distributions of these 3 α-emitting daughter nuclides of ^{225}Ac are no longer determined by the carrier molecule and thus may increase toxicity as compared with drugs carrying a single α-particle–emitting isotope. Therefore, estimating appropriate doses of ^{225}Ac from chelated ^{213}Bi or chemically conjugated ^{211}At data (both of which have been used in humans) might not be accurate. Difficulties may arise when estimating the impact of free ^{221}Fr, ^{217}At, and ^{213}Bi for therapeutic efficacy or for toxicity, as there are no previous data available for the first 2 elements, and minimal data for bismuth. Studies with longer-lived bismuth isotopes show that a considerable fraction of bismuth will be accumulated and excreted in the kidneys (*21*). Thus, renal toxicity in this study was an expected finding. The data also suggest that toxicity will be determined to a major extent by the redistribution of ^{225}Ac daughters. Nearly half of the last α-emitting daughter nuclide (^{213}Bi) was cleared from the blood, indicating that redistribution of daughter nuclides occurred. Excretion of heavy metals can be enhanced by administration of chelators such as 2,3-dimercapto-1-propanesulfonic acid, ethylenediaminetetraacetic acid, DTPA, and dimercaptosuccinic acid (*22*). Therefore, similar methods might be beneficial to reduce toxicity.

In the 2 monkeys showing acute radiation nephritis, the estimated absorbed dose to the renal cortex (assuming lo-

TABLE 2
Dosimetry of Single Dose of ^{225}Ac-HuM195 Following Pharmacokinetics in Monkey 2

	No. of disintegrations (/37 kBq)				Absorbed dose (Gy/37 kBq)			
	Blood (Bq-s/kg)		RC (Bq-s)		Blood		RC	
Isotope	A	B	A	B	A	B	A	B
^{225}Ac	1.5×10^{10}	1.5×10^{10}	0	0	0.014	0.014	0	0
^{221}Fr	1.5×10^{10}	8.1×10^{9}	0	3.2×10^{9}	0.016	0.008	0	0.05
^{217}At	1.5×10^{10}	8.1×10^{9}	0	3.2×10^{9}	0.017	0.009	0	0.06
^{213}Bi	8.1×10^{9}	8.1×10^{9}	3.2×10^{9}	3.2×10^{9}	0.011	0.011	0.07	0.07
Total	5.4×10^{10}	4.0×10^{10}	3.2×10^{9}	9.6×10^{9}	0.058	0.042	0.07	0.17

RC = renal cortex portion of kidney.
A and B refer to radionuclide decay assumptions A and B in text.

UH & EURATOM Ex. 2021-008
Fusion v. Universität Heidelberg, et al.
IPR2023-00551

calization of ^{221}Fr and subsequent daughters to the renal cortex) was 9–13 Gy. The renal cortex was chosen as the primary target tissue since there is evidence that heavy metals localize to this portion of the kidney (*14*). It is important to note that the absorbed-dose estimates are based on assuming a uniform deposition of α-particle energy throughout the renal cortex mass. As with almost all absorbed-dose calculations, this is a necessary oversimplification in the absence of detailed microbiodistribution data. The implications and possible errors associated with such an oversimplification, however, are profound for α-particle emitters due to their high potency and short range. Depending on the actual microbiodistribution, the biologic effects could be substantially greater or smaller than one might expect from an estimated absorbed dose of 13 Gy. In humans, the tolerated dose of external beam radiation yielding radiation nephritis in 50% of humans within 5 y ($TD_{50/5}$) is 28 Gy (*17*). Assuming that a relative biologic effectiveness (RBE) factor of 5 applies, the RBE-adjusted absorbed-dose range of 45–65 Gy to the monkey renal cortex is consistent with the toxicity observed in the monkeys.

CONCLUSION

In this study we showed that ^{225}Ac-HuM195 can safely be administered at a dose level of 28 kBq/kg, whereas dose escalation caused significant toxicity at cumulative doses of 215–370 kBq/kg. For repeated treatment cycles, pharmacokinetics did not appear to be influenced by an immune response against HuM195. However, antibody production against xenogeneic monoclonal antibodies can occur at any time during the treatment. Significant human antibody response to HuM195 has not been reported. In humans, the biologic $t_{1/2}$ of HuM195 is 4–5 times shorter than that in monkeys because of rapid targeting of the antibody-based drug and subsequent cellular internalization of the immune complex. Therefore, we assume that a dose level of at least 28 kBq/kg may be administered with tolerable acute side effects.

ACKNOWLEDGMENTS

We thank Krista LaPerle, VMD, PhD, and Hai Nguyen, VMD, for careful review and valuable discussion of histopathology. We also thank Laike Stewart, VMD, and Felix Homberger, VMD, PhD, for helpful advice. The help from Ron Finn, PhD, Jing Qiao, Michael Curcio, and Catalina Cabassa for preparing the radiopharmaceuticals and George Gonzales and Donna Ortiz for excellent care of the animals is acknowledged. This work was supported by National Institutes of Health grants P01 33049 and R01 55349; the Steps for Breath Fund; William H. Goodwin and Alice Goodwin and the Commonwealth Cancer Foundation for Research and the Experimental Therapeutics Center of MSKCC; and the Doris Duke Charitable Foundation.

REFERENCES

1. Cheson BD. Radioimmunotherapy of non-Hodgkin lymphomas. *Blood.* 2003; 101:391–398.
2. Richman CM, DeNardo SJ. Systemic radiotherapy in metastatic breast cancer using ^{90}Y-linked monoclonal MUC-1 antibodies. *Crit Rev Oncol Hematol.* 2001; 38:25–35.
3. Zalutsky MR, Zhao XG, Alston KL, Bigner D. High-level production of alpha-particle-emitting ^{211}At and preparation of ^{211}At-labeled antibodies for clinical use. *J Nucl Med.* 2001;42:1508–1515.
4. Gotthardt M, Fischer M, Naeher I, et al. Use of the incretin hormone glucagon-like peptide-1 (GLP-1) for the detection of insulinomas: initial experimental results. *Eur J Nucl Med Mol Imaging.* 2002;29:597–606.
5. McDevitt MR, Finn RD, Ma D, Larson SM, Scheinberg DA. Preparation of alpha-emitting ^{213}Bi-labeled antibody constructs for clinical use. *J Nucl Med.* 1999;40:1722–1727.
6. Azria D, Jacot W, Prost P, et al. Gemcitabine and ionizing radiations: radiosensitization or radio- chemotherapy combination [in French]. *Bull Cancer.* 2002; 89:369–379.
7. DeNardo SJ, Williams LE, Leigh BR, Wahl RL. Choosing an optimal radioimmunotherapy dose for clinical response. *Cancer.* 2002;94:1275–1286.
8. Jurcic JG, Larson SM, Sgouros G, et al. Targeted alpha particle immunotherapy for myeloid leukemia. *Blood.* 2002;100:1233–1239.
9. McDevitt MR, Scheinberg DA. Ac-225 and her daughters: the many faces of Shiva. *Cell Death Differ.* 2002;9:593–594.
10. McDevitt MR, Ma D, Lai LT, et al. Tumor therapy with targeted atomic nanogenerators. *Science.* 2001;294:1537–1540.
11. Zidenberg-Cherr S, Clegg MS, Parks NJ, Keen CL. Localization of bismuth radiotracer in rat kidney following exposure to bismuth. *Biol Trace Elem Res.* 1989;19:185–194.
12. McDevitt MR, Ma D, Simon J, Frank RK, Scheinberg DA. Design and synthesis of ^{225}Ac radioimmunopharmaceuticals. *Appl Radiat Isot.* 2002;57:841–847.
13. National Research Council. *Guide for the Care and Use of Laboratory Animals*. NIH publication 85-23. Bethesda, MD: U.S. Department of Health and Human Services, National Institutes of Health; 1985.
14. Russ GA, Bigler RE, Tilbury RS, Woodard HQ, Laughlin JS. Metabolic studies with radiobismuth. I. Retention and distribution of ^{206}Bi in the normal rat. *Radiat Res.* 1975;63:443–454.
15. Dubin NH, Blake DA, DiBlasi MC, Parmley TH, King TM. Pharmacokinetic studies on quinacrine following intrauterine administration to cynomolgus monkeys. *Fertil Steril.* 1982;38:735–740.
16. International Commission on Radiological Protection. *Report of the Task Group on Reference Man*. ICRP Publication 23. New York, NY: Pergamon Press; 1975:280–325.
17. Bouchet LG, Bolch WE, Blanco HP, et al. MIRD Pamphlet No. 19: Absorbed fractions and radionuclide S values for six age-dependent multiregion models of the kidney. *J Nucl Med.* 2003;44:1113–1147.
18. Caron PC, Dumont L, Scheinberg DA. Supersaturating infusional humanized anti-CD33 monoclonal antibody HuM195 in myelogenous leukemia. *Clin Cancer Res.* 1998;4:1421–1428.
19. Stephen C, Peiper RGA. CD33 Cluster Workshop Report. In: Schlossman SF, Boumsell L, Gilks W, et al., eds. *Leukocyte Typing V.* Oxford, U.K.: Oxford University Press; 1995:837–840.
20. Sgouros G, Jureidini IM, Scott AM, Graham MC, Larson SM, Scheinberg DA. Bone marrow dosimetry: regional variability of marrow-localizing antibody. *J Nucl Med.* 1996;37:695–698.
21. Newton D, Talbot RJ, Priest ND. Human biokinetics of injected bismuth-207. *Hum Exp Toxicol.* 2001;20:601–609.
22. Jones SB, Tiffany LJ, Garmestani K, Gansow OA, Kozak RW. Evaluation of dithiol chelating agents as potential adjuvants for anti-IL-2 receptor lead or bismuth alpha radioimmunotherapy. *Nucl Med Biol.* 1996;23:105–113.

UH & EURATOM Ex. 2021-009
Fusion v. Universität Heidelberg, et al.
IPR2023-00551